

Statistics of Voronoi polyhedra in a model silicon glass

K. Tsumuraya and K. Ishibashi

School of Science and Technology, Meiji University, Higasi-mita, Tama, Kawasaki, Kanagawa, 214, Japan

K. Kusunoki

National Research Institute for Metals, Nakameguro, Meguro-ku, Tokyo, 153 Japan

(Received 23 July 1992; revised manuscript received 17 September 1992)

We clarify the local structure in a model silicon glass by use of Voronoi-polyhedron analysis. The glass is produced by molecular dynamics with a Stillinger-Weber potential. The atoms in the glass are nearly distinguishable: there are about 200 types in the system with 216 atoms. The analysis clarifies that the polyhedra are formed by a small number of large-area polygons or by a large number of small-area polygons. This feature is different from those in Lennard-Jones glasses or metallic glasses and is attributed to the loose-packed structure even in the glass state, in which the atoms still have directional bonding. The variety of Voronoi signatures that appear in the covalently bonded glass can be simplified mainly into two types of signatures by constructing the polyhedra by use of the bonding atoms.

I. INTRODUCTION

The study of the structure of random systems has received great interest from a statistical point of view. Molecular-dynamics methods have been extensively used for modeling the random systems. In order to identify the local structures in the model random systems various methods have been used such as Voronoi-polyhedron analysis,¹⁻¹² bond orientational order parameters,^{13,14} and a method by Jónsson and Andersen.¹⁵ Among these, the Voronoi-polyhedron analysis gives very useful information about individual atoms, since it gives a specified signature for each atom. The concept of the polyhedron was proposed by Voronoi.¹⁶ Bernal¹⁷ has modeled a random structure by use of ball bearings and Finney¹ has analyzed the structure. Tanemura *et al.*² later clarified the nucleation process for supercooled model liquids using this analysis. Since then, the method has been widely used to analyze the local structures in random systems such as sodium,³⁻⁶ rubidium,⁷⁻⁹ Lennard-Jones materials,⁹⁻¹¹ and soft-core systems.² The crystallization processes for supercooled liquids have also been analyzed.^{2,12} All of the above are close-packed systems. In these glass systems this analysis has clarified that the most abundant polygon is the pentagon, and the polyhedron with 14 faces appears to be the most abundant. These results are insensitive to the potentials used as long as the system is close-packed.

Covalently bonded systems such as silicon and germanium easily vitrify into glassy states. The structure of the model silicon glass has been clarified by use of pair-distribution functions (PDF's),¹⁸⁻²⁵ static structure factors,^{18-21,24,26} and information concerning the number of bonds,¹⁸⁻²³ bond angles,^{20,21,24} dihedral angle distribution,²¹ and the local stability of atoms in the glasses.^{19-22,27} It has been found that the average number of bonds, bond angles, and dihedral angles are almost the same as those in the crystalline state. As far as we know, there has been no study on the application of the

Voronoi-polyhedron analysis to loosely-packed glass systems. In the present paper we clarify the local structures of a model silicon glass and compare with those in the close-packed glass systems. In Sec. II, the computational method will be described. In Sec. III, we will present the structures of the model glass. In Sec. IV, we will discuss the origin of the features, which are clarified with the Voronoi-polyhedron analysis. In Sec. V, our conclusions will be presented.

II. COMPUTATIONAL METHODS

There are a variety of potentials²⁸⁻³² for simulating the silicon system. Keating³¹ has proposed a harmonic potential for the crystal system. Baraff, Kane, and Schlüter,³² have modified the potential by incorporating the results of electronic total-energy calculations. Stillinger and Weber¹⁸ have proposed a potential for the system, which comprises two- and three-body terms. Later Tersoff,²⁸ Biswas and Hamann,²⁹ and Kaxiras and Pandey³⁰ also proposed potentials for Si. Among them, the Stillinger-Weber (SW) potential has been widely used for the simulations not only in the liquid^{14,18,23} but also to study crystal growth from supercooled liquids²⁵ and via deposition.³³ Glassy structures obtained by cooling,^{20,23,34} are not well described by the original SW potential. The pair-distribution functions (PDF) do not coincide with those obtained by experiment. In order to avoid this difficulty, some methods have been presented. One of these involves increasing the volume of the simulation box.¹⁹ The other involves increasing the strength of the three-body term of the SW potential to force tetrahedral bonding upon cooling.^{20,23} The third is to use a hybrid method of molecular dynamics and the Metropolis algorithm by rearranging the atom positions of the diamond cubic structure.³⁵ Based on these earlier works, we use the modified potential to realize the correct glass structure.

The system contains 216 atoms in a cubic cell and has

periodic boundary conditions in three dimensions. We have used the Andersen³⁶ constant pressure form of molecular dynamics. The external pressure is fixed at zero throughout the series of simulations. The unit of length $\sigma = 2.0951 \times 10^{-10}$ m and energy $\epsilon = 3.4723 \times 10^{-19}$ J. The units σ and ϵ are chosen to be the minimum distance and the energy of the two-body term of the potential. The initial edge length L of the cubic cell is 7.75049σ and unit of time $\tau = 7.6634 \times 10^{-14}$ s. The equation of motion has been integrated by use of Beeman's algorithm,³⁷ with an integration time step $\Delta t = 5 \times 10^{-3}\tau$. The velocities of atoms have been controlled by a modified momentum scaling method.^{3-7,38}

We prepared the glass as follows. (1) We arranged the atoms randomly in the cell. We stabilized the system for 10^4 steps at 1850 K with the original SW potential in which the coefficient $\lambda = 21$ for the three-body term. This temperature is higher than the melting temperature¹⁹ 1750 K of the model silicon system. The liquid state was confirmed by monitoring the mean-square displacement of the atoms. (2) The coefficient λ was changed continuously from 21 to 31 for 5000 steps. During this process the density decreased from $0.490\sigma^{-3}$ to $0.420\sigma^{-3}$. We then stabilized the system for 5000 steps at that temperature. The value of $\lambda = 31$ was used to simulate the correct glass structure of the silicon glass.²⁰ (3) We then cooled the liquid to 300 K with a continuous cooling method,^{5,39-41} with a rate of 0.0155 K for every step. This corresponds to a cooling rate of 4.05×10^{13} K s⁻¹. During this process the density increased from $0.420\sigma^{-3}$ to $0.430\sigma^{-3}$. (4) The coefficient λ was continuously reduced to 21 for 2000 steps at 300 K in order to relax the structure. During this time, the density increased to $0.445\sigma^{-3}$. We continued to simulate the system for 48 000 steps in order to achieve stabilization. The density increased to $0.446\sigma^{-3}$. We used the last 10^4 steps to obtain the statistical average of the structures.

III. RESULTS

A. Mean-square displacement of atoms

In order to examine the movements of atoms at 300 K, we have measured the mean-square displacements of the atoms, $\langle [r_i(t) - r_i(0)]^2 \rangle$. The displacement at 1850 K increased quadratically with time in the initial region and then increases linearly with time there indicating that the system is in the liquid state. The quadratic increment appeared in the initial region and is attributed to the thermal vibration of atoms prior to migration.⁴² The slope at 300 K, however, was zero, which indicates that no long-range movement of atoms occurs at 300 K, except for the local vibrations. We will examine statistically the local structures around atoms at this temperature in the following section.

B. Pair-distribution function and number of bonds

Figure 1 shows the radial distribution $g(r)$ of atoms in the condensed system, averaged every 100 steps. The first peak is located at $r = 1.14\sigma$ and the second peak at $r = 1.83\sigma$. The peak positions and heights of $g(r)$ coin-

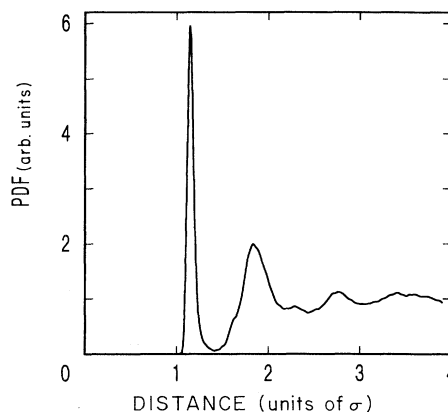


FIG. 1. Pair-distribution function at 300 K.

cide with those of earlier PDF's.^{19,20} The peak position of the first peak occurs nearer the origin (by 0.05σ) than that of the PDF of Wooten, Winer, and Weaire.³⁵ Their glass was formed by the hybrid method by use of the Keating potential³¹ and gave a Gaussian line broadening.³⁵ Here let us examine the bond statistics of atoms in the glassy state. The PDF has shown a deep first minimum at $r = 1.41\sigma$ just outside of the first peak as shown in Fig. 1. We use this distance as a cutoff for the bonding statistics. The distribution of bond angles made by two bonds of a triplet are shown in Fig. 2. As expected the most abundant angle is 108° and the average angle is 108.22° , which is close to the value of 109.47° found in the crystalline state. Table I shows the comparison of the angles and the standard deviations of the broadnesses among the earlier works. The present distribution is the same as those of the earlier works.^{20,23}

Table II shows the fractions of atoms with various number of bonds in the range of the first minimum of PDF. The most probable number of bonds is four and the average number of bonds is 4.13. Earlier works have shown various values for the model silicon glasses such as

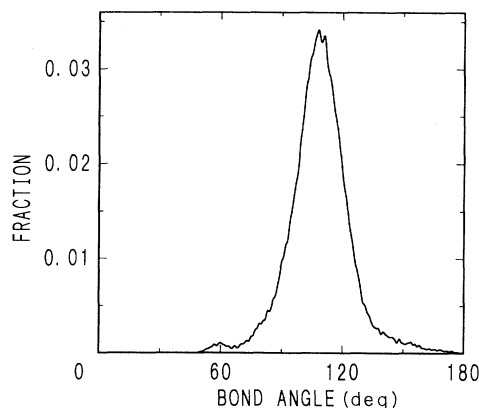


FIG. 2. Bond-angle distribution for the glassy state.

TABLE I. The average bond angles and the broadnesses among the model silicon glasses.

	Present work ($T=300$ K)	Luedtke and Landman ^a ($T=300$ K)	Štich, Car, and Parrinello ^b ($T=300$ K)
Average bond angle	108.22°	108.3°	108.32°
Broadness ^c	15.2	14.7	15.5

^aReference 20 calculated by SW potential.

^bReference 21 calculated by *ab initio* molecular-dynamics method.

^cStandard deviation of their distributions.

4.12,^{19,20} 4.10,²³ 4.0–4.05,²⁴ and 4.03.²¹ The present fractions of atoms and the average number of bonds are almost the same values as those earlier works.^{20,21,23} Thus the crystal-like bonding nature is still realized even in the glass state.

C. Voronoi-polyhedron analysis

In order to examine the local environments around each atom in the glass, we have used a Voronoi-polyhedron analysis. This analysis is a useful method to identify the near-neighbor environments around each atom in the condensed systems.^{1–12} The polyhedron is constructed by the following procedure: A bisection plane is formed from a central atom to one of the coordinated atoms in the system. The planes are formed between the central atom and all the neighboring atoms around it. The planes form a variety of shapes of polygons around the central atom. The polyhedron consists of the polygons which are the closest to the central atom. We call it the Voronoi polyhedron. The polyhedron corresponds to the Wigner-Seitz cell in the crystalline state. Each polyhedron is identified by a signature ($n_3, n_4, n_5, \dots, n_j, \dots$), where n_j is the number of j -edged polygons on the polyhedron.

We have examined the signatures of each atom in the glass state. There are over 200 different signatures every simulation step in our system of 216 atoms, indicating the appearance of signatures which are almost independent. In contrast to our studies on metal sodium glass,^{3–6} we cannot analyze the glass state by classifying them into de-

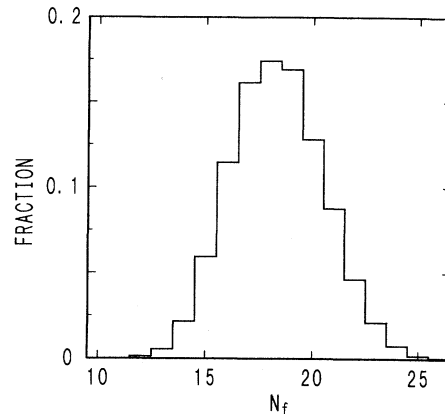


FIG. 3. Distribution of the number N_f of faces on each polyhedron in the glassy state.

creasing order of abundance. For sodium glass, there were 129 signatures in our 864 atom glass; the most abundant signature of which corresponds to 0.10 of the total.

In order to characterize the shapes of the Voronoi polyhedra, we first counted the number N_f of faces on each polyhedron. Figure 3 shows the results for N_f . The distribution ranged from $N_f=11$ –26 and is a broad and almost Gaussian function. The average $N_f=18.35$ with a standard deviation of 2.17. The most probable number of faces is 18. For the sodium glass,^{3–6} the range of the distribution was only from 12 to 17, the most probable number of faces was 14, and the standard deviation was 1.13. These parameters are greater for the present glass than for the sodium glass, and indicate a variety of local environments of atoms in the present glass.

We have also counted the number N_e of edges on each polygon, and have examined the fraction of N_e . Figure 4(a) shows the fraction as a function of N_e . The distribution has a sharp peak at $N_e=4$ and a subpeak at $N_e=9$. The distribution is completely different from that which appeared in the sodium glass,^{3–6} which showed a single peak with maximum at $N_e=5$. In order to clarify the distribution, we have identified the polygons which were formed by the bonding atoms and have shown their fractions in Fig. 4(b) as a solid line. We have also shown the fraction of N_e for the nonbonding atoms as a broken line.

TABLE II. Fractions of Si atoms with various numbers of bonds.

Number of atoms	Present work ($T=300$ K)	Luedtke and Landman ^a ($T=300$ K)	Broughton and Li ^b ($T=754$ K)	Štich, Car, and Parrinello ^c ($T=300$ K)
3	0.006	0.005	0.012	0.002
4	0.861	0.878	0.866	0.966
5	0.133	0.115	0.118	0.032
6	0.001	0.003	0.002	
Average	4.14	4.12	4.10	4.03

^aReference 20 calculated by SW potential.

^bReference 23 calculated by a method by Wooten, Winer, and Weaire (Ref. 35).

^cReference 21 calculated by *ab initio* molecular-dynamics method.

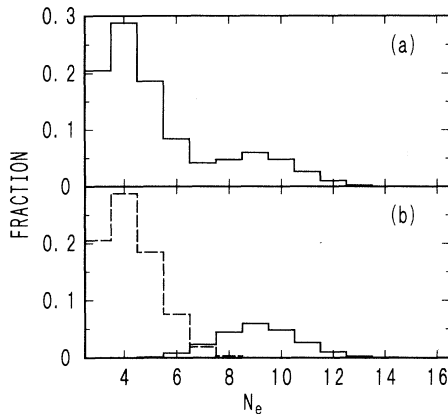


FIG. 4. Distributions of the number N_e of edges for polygons on all the polyhedra in the glassy state: solid line in (a) is the distribution of the polygons with number N_e formed by all the coordinated atoms around each atom, the solid line in (b) is for the bonding atoms, and the broken line in (b) is for the nonbonding atoms.

The peak in Fig. 4(a) corresponds to the fraction of N_e formed by nonbonding atoms and the subpeak to the bonding atoms. Let us specify the polygons on the Voronoi polyhedra formed by bonding atoms and those by nonbonding atoms. We define these the bonding polygons and the nonbonding polygons.

We have examined the shape of polyhedra appearing in the glass. Figure 5 shows a typical shape of a polyhedron that has a signature (5,4,3,3,1,0,0,2,1). There are two distributions in n_j , i.e., one of them is a group of polygons with small area and the other is that with large area. Generally there are three parameters needed to identify the polygons on the polyhedron. These are the number N_e of edges, the area, and the distance from the central atom.

We have examined the average areas as a function of N_e . Figure 6 shows the results. The circles represent the average areas of polygons. The areas of the bonding polygons are also shown together with those of the nonbonding ones. Both areas increase linearly with increasing N_e . The areas of the bonding polygons approach the

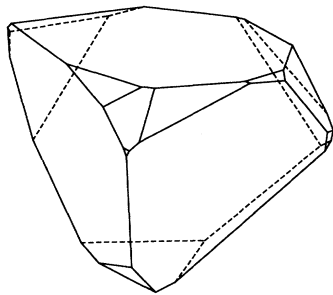


FIG. 5. The shape of a Voronoi polyhedron in the glassy state.

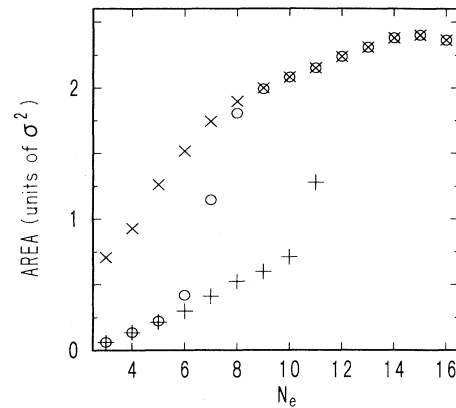


FIG. 6. The average surface areas of polygons on the Voronoi polyhedra as a function of the number N_e of edges on polygons: The plus represents the areas of surfaces formed by the bonding atoms, the cross represents the nonbonding atoms, and the circles represent the coordinated atoms.

average at the large- N_e region and those of nonbonding ones at the low- N_e region.

We have also examined the distance of polygons from the central atoms. Figure 7 shows the interatomic distances as a function of N_e together with the PDF shown in Fig. 1. The interatomic distances of 1.9σ , which are associated with the formation of the triangle $N_e=3$, are included in the second peak of the PDF and those less than 1.15σ with the formation of polygons with $N_e > 9$ in the first peak. This relation is a measure of the interatomic distances of the polygons on the polyhedron appearing in Fig. 5.

IV. DISCUSSION

In Sec. III, we have found that among the 216 atoms there are more than 200 types of signatures which had

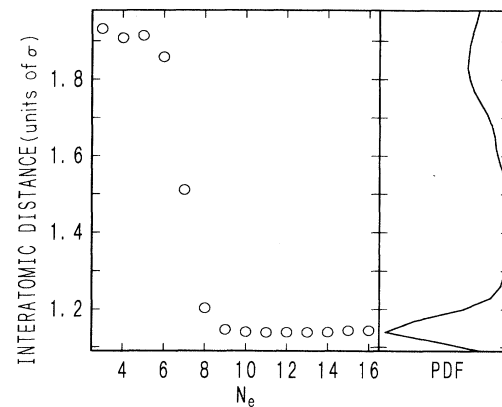


FIG. 7. The relation between the average interatomic distance and the number of edges of the polygons N_e on the bisection planes, which are formed from the central atoms to the coordinated atoms. The PDF appearing in Fig. 1 is shown for comparison.

only one atom, and 10 types of signatures which had two atoms, showing the independent appearance of the signatures. These features are in complete contrast to those in the sodium glass,³⁻⁶ Lennard-Jones glass,^{9,10} and rubidium glass.⁷⁻⁹ Here we discuss the reason for their appearance. In the case of sodium glass,³⁻⁶ there were 129 types of signature for the 864 atom system studied: The most abundant case had 80 atoms with the same signature. The second most abundant signature had almost the same number. The sum of the fractions up to the 13th signature accounted for 0.64 of the total. The average number of bond atoms in the first peak of the PDF was 12.96, which is greater than that in the present glass. The average number of polygons on the polyhedra was 13.87. The difference 0.91 between the numbers indicates that the contribution from the atoms outside of the first peak is small. In the case of the present glass the average bond angles is 108.22° and the average number of bonds is 4.13. This indicates that the bonding character is covalent even in the glass state and means that the atoms form directional bonding and a loose-packed structure even in the glass. The variety of signatures relates to the bonding. The average number of polygons on the Voronoi polyhedra was 18.35 from Fig. 3. The difference, 14.22, between the numbers is the contribution of the nonbonding atoms outside of the first peak of the PDF. Thus the bonding in the silicon glass is so directional that the nonbonding atoms contribute to the formation of the polygons.

The bisector planes formed by the nonbonding atoms cut those formed by the bonding atoms. Since the nonbonding atoms locate in the loose-packed space among the bonding atoms, there are a variety of cutting directions. The bonding polygons have large N_e and have been located in the large- N_e region as was shown in Fig. 4. On the contrary, the nonbonding atoms, which are located among the bonding atoms, form the polygons with small areas. Thus the number N_e of the bonding polygons increases and the nonbonding polygons have a small

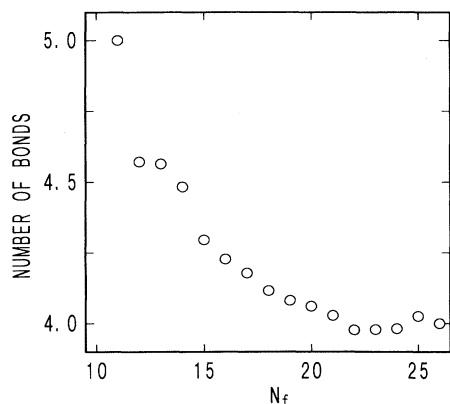


FIG. 8. The relation between the number of bonds and the total number of faces on the polyhedron N_f . The number N_f is a measure of contribution of the nonbonding atoms to the formation of the polyhedra.

TABLE III. Fractions of Voronoi polyhedra formed by nearest-neighbor atoms at 300 K.

Signature	Number of bonds	Fraction of atoms
(4,0,0)	4	0.8587
(2,3,0)	5	0.1325
(0,0,0) ^a	3	0.0056
(1,0,0) ^a	4	0.0020
(2,2,2)	6	0.0007
(0,6,0)	6	0.0002
(3,1,0) ^a	5	0.0001
(0,1,0) ^a	5	0.0001

^aNo polyhedron is constructed in these signatures.

number of edges. As a result the number of types of signatures increases.

In order to confirm this point, we have examined the relation between the number of bonds around each atom and the number N_f of each polyhedron. Figure 8 shows the average number of bonds as a function of N_f . The number N_f is a measure of contribution of the nonbonding atoms to the formation of the polyhedra. The central atoms with a large number of bonding atoms produce the polyhedra with low N_f , while the atoms with low number of bonding atoms, four for example, produces the polyhedra with large N_f . The number N_f increases with decreasing number of bonds, which is a measure of the directional bonding. Such a situation produces the shape of the polyhedron shown in Fig. 5. Thus the decrease of the number of bonds results in space around the central atoms; the nonbonding atoms locate in the space, and the bisector planes produced by the nonbonding atoms cut bisector planes formed by the bonding atoms. This is the reason why the atoms with a low number of bonds produce polyhedra with large N_f .

In order to eliminate the effect of faces with small areas, we formed the Voronoi polyhedra with the atoms in the first peak of the PDF $g(r)$ shown in Fig. 1. The fractions of signatures are shown in Table III in the order of decreasing fraction. Almost all the polyhedra are classified into (4,0,0) and (2,3,0) signatures. The sum of their fractions is 0.99. Figure 9 shows a typical shape of the polyhedra with (4,0,0) and (2,3,0) signatures. In the (2,3,0) polyhedron there are two triangles. Each triangle is surrounded by three squares. The smaller triangle is formed by cutting one of the vertices of the (4,0,0)

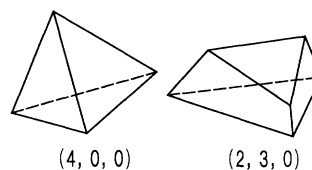


FIG. 9. Typical shapes of the (4,0,0) and (2,3,0) Voronoi polyhedra.

polyhedron in the figure. Thus the variety of Voronoi signatures appeared in the covalently bonded glass can be simplified mainly into two types of signatures by constructing the polyhedra by use of the bonding atoms.

V. CONCLUSION

We have clarified the local structure in a model silicon glass produced by the molecular-dynamics method with the Stillinger-Weber potential. The local structure has been analyzed by use of the Voronoi-polyhedron method. Each atom has an almost independent signature, in contrast to the appearance of many common signatures in the close-packed glasses. The origin of this observation has been analyzed statistically. Directional bonding exists even in the glass state. The bonding atoms form a loose-packed structure and the nonbonding atoms locate

in the spaces, resulting in a large number of polygons on the polyhedra. We have eliminated the small areas from the Voronoi polyhedra by constructing the faces with the bonding atoms. The elimination results in the simplification of the polyhedra into the (4,0,0) and (2,3,0) signatures.

ACKNOWLEDGMENTS

The authors thank the Supercomputer Facility at the School of Science and Technology, Meiji University for the use of their ETA-10 computer, the Computer Center, Meiji University for the use of their VP-2200 supercomputer, and the Computer Center, Institute for Molecular Science, Okazaki National Research Institute for the use of their HITAC M-680H and S-820/80 computers.

-
- ¹J. L. Finney, Proc. R. Soc. London, Ser. A **319**, 479 (1970).
²M. Tanemura, Y. Hiwatari, H. Matsuda, T. Ogawa, N. Ogita, and A. Ueda, Prog. Theor. Phys. **58**, 1079 (1977).
³M. S. Watanabe and K. Tsumuraya, J. Chem. Phys. **87**, 4891 (1987).
⁴K. Tsumuraya and M. S. Watanabe, J. Chem. Phys. **92**, 4983 (1990).
⁵T. Kondo, K. Tsumuraya, and M. S. Watanabe, J. Chem. Phys. **93**, 5182 (1990).
⁶T. Kondo and K. Tsumuraya, J. Chem. Phys. **94**, 8220 (1991).
⁷M. Tanaka, J. Phys. Soc. Jpn. **55**, 3108 (1986).
⁸N. N. Medvedev, J. Phys. Condens. Matter **2**, 9145 (1990).
⁹M. Tanaka, J. Phys. Soc. Jpn. **55**, 3428 (1986).
¹⁰M. Kimura and F. Yonezawa, J. Non-Cryst. Solids **61 & 62**, 535 (1984); *Topological Disorder in Condensed Matter*, edited by F. Yonezawa and T. Ninomiya (Springer, Berlin, 1983), p. 80.
¹¹Y. I. Naberukhin, V. P. Voloshin, and N. N. Medvedev, Mol. Phys. **73**, 917 (1991).
¹²C. S. Hsu and A. Rahman, J. Chem. Phys. **70**, 5234 (1979); *ibid.* **71**, 4974 (1979).
¹³P. J. Steinhardt, D. R. Nelson, and M. Ronchetti, Phys. Rev. B **28**, 784 (1983).
¹⁴Z. Q. Wang and D. Stroud, J. Chem. Phys. **94**, 3896 (1991).
¹⁵H. Jónsson and H. C. Andersen, Phys. Rev. Lett. **60**, 2295 (1988).
¹⁶G. F. Voronoi, J. Reine Angew. Math. **134**, 198 (1908).
¹⁷J. D. Bernal, Proc. R. Soc. London, Ser. A **280**, 299 (1964).
¹⁸F. H. Stillinger and T. A. Weber, Phys. Rev. B **31**, 5262 (1985).
¹⁹M. D. Kluge, J. R. Ray, and A. Rahman, Phys. Rev. B **36**, 4234 (1987).
²⁰W. D. Luedtke and U. Landman, Phys. Rev. B **37**, 4656 (1988); **40**, 1164 (1989).
²¹I. Štich, R. Car, and M. Parrinello, Phys. Rev. B **44**, 11 092 (1991).
²²F. Buda, G. L. Chiarotti, I. Štich, R. Car, and M. Parrinello, J. Non-Cryst. Solids **114**, 7 (1989).
²³J. Q. Broughton and X. P. Li, Phys. Rev. B **35**, 9120 (1987).
²⁴R. Biswas, G. S. Grest, and C. M. Soukoulis, Phys. Rev. B **36**, 7437 (1987).
²⁵G. H. Gilmer, M. H. Grabow, and A. F. Bakker, *Proceedings of the International Workshop on Computational Materials in Science*, edited by A. Yoshikawa (National Research Institute for Metals, Japan, 1990), p. 27.
²⁶J. M. Holender and G. J. Morgan, J. Phys. Condens. Matter **3**, 1947 (1991).
²⁷U. Landman, W. D. Luedtke, M. W. Ribarsky, R. N. Barnett, and C. L. Cleveland, Phys. Rev. B **37**, 4637 (1988); **37**, 4647 (1988).
²⁸J. Tersoff, Phys. Rev. Lett. **56**, 632 (1986); Phys. Rev. B **37**, 6991 (1988); **38**, 9902 (1988).
²⁹R. Biswas and D. R. Hamann, Phys. Rev. B **36**, 6434 (1987).
³⁰E. Kaxiras and K. C. Pandey, Phys. Rev. B **38**, 12 736 (1988).
³¹P. N. Keating, Phys. Rev. **145**, 637 (1966); *ibid.* **149**, 674 (1966).
³²G. A. Baraff, E. O. Kane, and M. Schlüter, Phys. Rev. B **21**, 5662 (1980).
³³W. D. Luedtke and U. Landman, Phys. Rev. B **40**, 11 733 (1984).
³⁴K. Ding and H. C. Andersen, Phys. Rev. B **34**, 6987 (1986).
³⁵F. Wooten, K. Winer, and D. Weaire, Phys. Rev. Lett. **54**, 1392 (1988).
³⁶H. C. Andersen, J. Chem. Phys. **72**, 2384 (1980).
³⁷P. Schofield, Comput. Phys. Commun. **5**, 17 (1973); D. Bee-man, J. Comput. Phys. **20**, 130 (1976).
³⁸M. Tanaka, J. Phys. Soc. Jpn. **51**, 3802 (1982).
³⁹J. R. Fox and H. C. Andersen, Ann. N.Y. Acad. Sci. **371**, 123 (1981); J. Phys. Chem. **88**, 4019 (1984).
⁴⁰R. D. Mountain and P. K. Basu, J. Chem. Phys. **78**, 7318 (1983); A. C. Brown and R. D. Mountain, *ibid.* **80**, 1263 (1984); R. D. Mountain and A. C. Brown, *ibid.* **80**, 2730 (1984).
⁴¹K. Shinjo, J. Chem. Phys. **90**, 6627 (1989).
⁴²M. Tanaka, Y. Fukui, and S. Takeuchi, J. Jpn. Inst. Metals **37**, 907 (1973).